

## Path-integral Monte Carlo method in quantum statistics for a system of $N$ identical fermions

A. P. Lyubartsev and P. N. Vorontsov-Velyaminov

*Scientific Research Institute of Physics, St. Petersburg State University, 198904, St. Petersburg, Russia*

(Received 18 February 1993)

A rigorous expression for the partition function of  $N$  identical fermions with spin  $\frac{1}{2}$  is obtained in a form suitable for a path-integral Monte Carlo (PIMC) simulation of a many-electron system at a finite temperature. A sum over permutations is reduced to a sum over classes with readily determinable factors. A distribution over projections and values of the total spin is also obtained, enabling PIMC calculations of spin-dependent quantities. A MC algorithm is proposed which accounts simultaneously for all types of trajectory linkages. A test calculation, four electrons in a spherical cavity with a radius of 1 nm at a temperature of 300–2000 K, is performed.

PACS number(s): 03.65.Ca, 05.30.-d, 02.70.Lq, 05.70.Ce

### I. INTRODUCTION

A Monte Carlo (MC) method developed for classical statistics was successfully applied in recent decades in computer simulations of a large variety of molecular systems. However, real atoms and molecules in fact are complicated many-electron systems and their interaction cannot always be adequately described within a classical pair potential model even at room temperature. That is especially the case for dense plasmas in which atoms, molecules, and atomic and molecular ions coexist with the electron component. So there is a need to have an instrument for the quantitative description of systems taking explicit account of the quantum statistics of the electron subsystem at finite temperature.

There exists now a MC method for quantum systems using Feynman path integrals [1]—the path-integral Monte Carlo (PIMC) method. Its numerical implementation to a system of  $N$  distinguishable particles is based on a sublimit approximation to the Feynman integral for the partition function expressed as the trace of a product of high-temperature density matrices in the coordinate representation [2–5]. In this treatment each quantum particle is represented by a “ring polymer” whose elements are connected by harmonic forces. Interparticle interactions are expressed as interaction between “simultaneous” vertices, i.e., vertices with the same index.

In the simulations of real systems, quantum particles are usually either helium atoms [5] or electrons [6,7]. As far as an  $N$ -electron system is a system of identical fermions its treatment requires a strict account of permutation symmetry and spin statistics.

It is known that permutation symmetry leads to linked trajectories [1] and the antisymmetry of the  $N$ -electron wave functions results in the problem of alternating signs of weight functions in the PIMC method. Still not clear is the question of an adequate account of the spin statistics. As a result, until now no simulation scheme practically realizable for systems with a sufficiently large number of electrons had been suggested. In the existing papers there were carried out PIMC simulations for 1 or 2

electrons [6,7]. The most serious contribution to this problem was made in the work of Shevkunov [8] in which the Young diagram approach was used to account for the spin statistics of electrons.

The aims of this paper are (1) to give a strict formulation of the PIMC method for the system of  $N$  identical electrons (Sec. II) and (2) to try to construct a practically realizable computational scheme (Sec. III). In Sec. IV a test simulation for four electrons in a cavity is presented with a discussion of its results. A short conclusion is given in Sec. V.

### II. PARTITION FUNCTION OF THE $N$ -ELECTRON SYSTEM

#### A. Antisymmetric density matrix

Consider a system of  $N$  electrons in volume  $V$  and the external field  $\varphi(r)$ . Its Hamiltonian is

$$H(r_1, \dots, r_N) = - \sum_{i=1}^N \frac{\hbar^2}{2m} \Delta_{r_i} + \sum_{i=1}^N \varphi(r_i) + \sum_{\substack{i=2, j=1 \\ i > j}}^N \Phi(r_i - r_j), \quad (1)$$

$$\Phi(r_i - r_j) = \frac{e^2}{|r_i - r_j|}.$$

The external field can have the form

$$\varphi(r) = - \sum_k \frac{z_k e^2}{|r - R_k|},$$

where  $R_k$  are the nuclei coordinates and  $z_k$  are their charges.

It is known that the density matrix of the system of  $N$  spinless fermions  $\rho^A(r_1, \dots, r_N, r'_1, \dots, r'_N)$  can be expressed as antisymmetrical combinations of the density matrices of a system of  $N$  distinguishable particles  $\rho^D(r_1, \dots, r_N, r'_1, \dots, r'_N)$  [9]:

$$\rho^A(r_1, \dots, r_N, r'_1, \dots, r'_N) = (1/N!)^2 \sum_{\{P\}} \sum_{\{P'\}} \text{sgn}(P) \rho^D(P(r_1), \dots, P(r_N), P'(r'_1), \dots, P'(r'_N)), \tag{2}$$

where  $\rho^D(r_1, \dots, r_N, r'_1, \dots, r'_N)$  is expressed by

$$\rho^D(r_1, \dots, r_N, r'_1, \dots, r'_N) = \sum_i \psi_i(r_1, \dots, r_N) \exp(-\beta E_i) \psi_i^*(r'_1, \dots, r'_N),$$

$\{P\}$  is the multitude of all permutations of  $N$  elements,  $\text{sgn}(P)$  is the sign of the permutation  $P$ , and  $\{\psi_i\}$  is the full set of solutions of the Schrödinger equation

$$H \psi_i(r_1, \dots, r_N) = E_i \psi_i(r_1, \dots, r_N).$$

The density matrix of the system of  $N$  distinguishable particles can be readily expressed by the path integrals in the form suitable for computer simulations [2–5].

According to the general scheme of the quantum-field-theory formalism [9,10], for a system of particles with spin  $s$  we should replace particle coordinates  $\{r_i\}$  by  $x_i = \{r_i, \sigma_i\}$  and  $\int dr$  by  $\sum_\sigma \int dr$ , where  $\sigma_i$  are spin projections. For a single particle with a spin-independent Hamiltonian it is possible to write

$$\rho(x, x') = \rho_0(r, r') \delta(\sigma, \sigma')$$

[ $\rho_0(r, r')$  is the coordinate part of the density matrix]. Accordingly, for  $N$  distinguishable particles with a spin-independent Hamiltonian,

$$\rho^D(x_1, \dots, x_N, x'_1, \dots, x'_N) = \rho_0^D(r_1, \dots, r_N, r'_1, \dots, r'_N) \delta(\sigma_1, \sigma'_1) \cdots \delta(\sigma_N, \sigma'_N). \tag{3}$$

Substituting (3) into (2) we obtain the expression for the partition function of the  $N$ -electron system, which is the trace of the antisymmetric density matrix:

$$Z = \text{Tr}(\rho^A) = (1/N!) \int dr_1 \cdots dr_N \sum_{\{P\}} \text{sgn}(P) K(P) \rho_0^D(r_1, \dots, r_N, P(r_1), \dots, P(r_N)), \tag{4}$$

where

$$K(P) = \sum_{\sigma_1, \dots, \sigma_N = \pm \frac{1}{2}} \delta(\sigma_1, P(\sigma_1)) \cdots \delta(\sigma_N, P(\sigma_N)) \tag{5}$$

is the spin factor contributing to the partition function. The first sum over permutations in formula (2) gives  $N!$  after integration. In the absence of spin,  $K(P) = 1$  and we come back to the known expressions (see, e.g., [9], Chap. 2).

**B. Path integrals and reduction to a sum over classes**

It is known that the density matrix for  $N$  distinguishable particles can be expressed as a path integral [1]:

$$\rho_0^D(r_1, \dots, r_N, r'_1, \dots, r'_N) = \lim_{J \rightarrow \infty} \int \prod_{i=1}^N dq_i(1) \cdots dq_i(J) (J/\lambda_i^2)^{3JN/2} \exp \left[ - \sum_{j=1}^J \sum_{i=1}^N \left\{ (\pi J/\lambda_i^2) [q_i(j+1) - q_i(j)]^2 \right\} - (\beta/J) \sum_{j=1}^J U\{q_i(j)\} \right], \tag{6}$$

where

$$U\{q_i(j)\} = \sum_i \phi(q_i(j)) + \sum_{i>k} \Phi(q_i(j) - q_k(j)).$$

Integration is made over the trajectories  $q_i(j)$  ( $i$  is the index of a particle,  $j$  is the index of a trajectory vertex), with the origins in points  $q_1(1) = r_1, \dots, q_N(1) = r_N$  and finishing in points  $q_1(J+1) = r'_1, q_N(J+1) = r'_N$  (see Fig. 1), where  $\lambda_i^2 = 2\pi\beta\hbar^2/m_i$  is the thermal wavelength for the  $i$ th particle.

In sublimit approximation  $J$  is taken to be a finite but large number. In the partition function  $Z = \text{Tr}(\rho^D)$  the initial points coincide with the final ones and hence a system of  $N$  closed trajectories with  $J$  intermediate vertices is formed.

In each term of the sum (4) the final point coincides with the initial one, though not necessarily for the same particle. Figure 2(a) demonstrates an example of such a

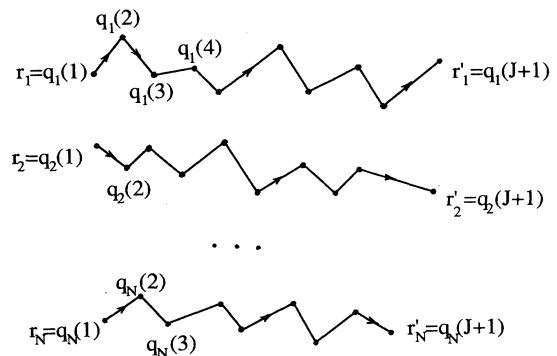


FIG. 1. Schematic representation of the trajectories for density matrix of  $N$  distinguishable particles.

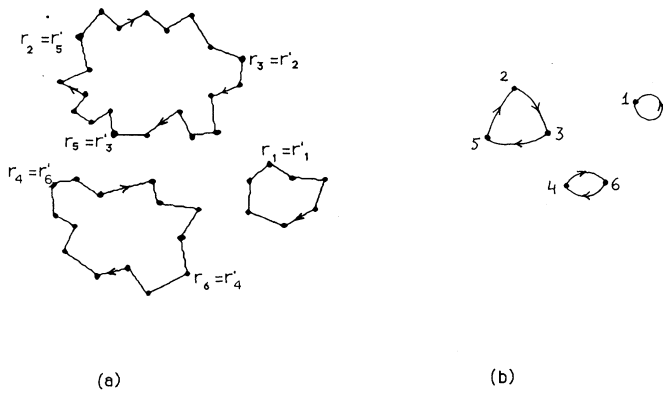


FIG. 2. Scheme of linked trajectories for  $N=6$  identical particles for permutation (135624). (a) Full set of trajectories with intermediate vertices. (b) Schematic diagram.

system of trajectories corresponding to  $N=6$ ,  $J=7$ , and to the permutation  $(123456) \rightarrow (135624)$ .

A certain structure of linked trajectories corresponds to each permutation. It can be presented by a diagram (or graph) with enumerated vertices, corresponding to initial points  $q_1(1)=r_1, \dots, q_N(1)=r_N$  and directed lines linking these points, omitting explicit presentation of intermediate points [Fig. 2(b)]. To each permutation there corresponds its own enumerated diagram; their total number is  $N!$ .

In order to perform MC simulation in the ensemble (4) it is necessary to organize a random walk both in coordinate  $\{q_i(j)\}$  space inside given volume  $V$  and in the space of all possible trajectory linkage schemes which correspond to all the permutations  $\{P\}$ .

As far as the full set of permutations is  $N!$  its complete account for large  $N$  is impossible. It is evident, however, that contributions of permutations differing only in enumeration of vertices in diagrams of the same topological structure are the same since all the expression is integrated over the set of coordinates  $\{q_i(j)\}$ . For example, the contribution of the permutation in Fig. 2 is equal to that of permutations  $(123456) \rightarrow (231546)$ ,

$$\sum_{\sigma_1, \dots, \sigma_6 = \pm \frac{1}{2}} (\delta(\sigma_1, \sigma_1))(\delta(\sigma_2, \sigma_3))(\delta(\sigma_3, \sigma_5))(\delta(\sigma_5, \sigma_2))(\delta(\sigma_4, \sigma_6))(\delta(\sigma_6, \sigma_4)).$$

It is evident that each group is nonzero only if all its spin variables are the same. So in each group it is possible to keep only one  $\delta$  symbol whose arguments can change independently, yielding a factor of 2 into the resulting product. So we get

$$K(P) = K(G) = 2^{\sum_{\nu} C_{\nu}(G)}, \quad (8)$$

i.e., 2 to the power of the complete number of cycles in the given class  $G$ . It should be noted here that the same result appears in the Handscomb MC method for the quantum Heisenberg model in the absence of an external field [12].

Expression (8) has a simple interpretation: "exchange interaction," which corresponds to the linked trajectories, can take place only among particles with the same spin projection (particles should be completely indistinguishable). Or, in other terms, the spin projection does not change along a closed trajectory.

The sign of a diagram can be also expressed by a simple formula:

$$\text{sgn}(G) = (-1)^{[G]}, \quad (9)$$

$$[G] = \sum_{\nu=1}^N (\nu-1)C_{\nu} = N - \sum_{\nu=1}^N C_{\nu}$$

TABLE I. Number of enumerated and nonenumerated diagrams for various  $N$ .

$N$	Number of enumerated diagrams ( $N!$ )	Number of nonenumerated diagrams $g(N)$
1	1	1
2	2	2
3	6	3
4	24	5
5	120	7
6	720	11
7	5 040	15
8	40 320	22
9	362 880	29

(123456)  $\rightarrow$  (152634), and some others. Such permutations, as is known from the group theory [11], belong to the same class of the permutation group. The sign (parity) of permutations belonging to the same class is also the same. The spin factors  $K(P)$  are the same also (they will be discussed and calculated below). Therefore it is possible to transfer from the sum over all permutations to the sum over classes of permutations (with corresponding coefficients) or correspondingly to the sum over nonenumerated diagrams. Their number grows with the increase of  $N$  comparatively slowly [8] (see also Table I).

Each nonenumerated graph can be labeled with a set of symbols  $\{C_{\nu}\}$ ,  $\nu=1, \dots, N$ , where  $C_{\nu}$  is the number of cycles of length  $\nu$ ,  $\sum_{\nu=1}^N \nu C_{\nu} = N$  [9]. The total number of diagrams of a given class  $G$  is [9,11]

$$n(G) = \frac{N!}{\prod_{\nu=1}^N (C_{\nu}! \nu^{C_{\nu}})}. \quad (7)$$

Now let us calculate the spin factors  $K(P)$  in the partition function (4). The sum (5) contains  $2^N$  terms corresponding to all possible sets of spin orientations. Group the  $\delta$  symbols that belong to the same cycles in a permutation  $P$ . For instance, for permutations of Fig. 2 it reads

[each closed trajectory of length  $\nu$  gives  $\text{sgn}(-1)^{\nu-1}$ ]. So the expression for the partition function of  $N$  identical particles (4) can be rewritten now as a sum over classes  $G$ :

$$\begin{aligned} Z &= (1/N!) \int dr_1 \cdots dr_N \sum_G n(G) K(G) \text{sgn}(G) \rho_0^D(r_1, \dots, r_N, P_G(r_1), \dots, P_G(r_N)) \\ &= (1/N!) \sum_G n(G) K(G) \text{sgn}(G) Z_{\text{cl}}(G), \end{aligned} \quad (10)$$

where

$$\begin{aligned} Z_{\text{cl}}(G) &= \int dr_1 \cdots dr_N \rho_0^D(r_1, \dots, r_N, P_G(r_1), \dots, P_G(r_N)) \\ &= (\lambda_J)^{-3JN} \int \prod_{i=1}^N dq_i(1) \cdots dq_i(J) \exp \left[ - \sum_{j=1}^J \sum_{i=1}^N \left\{ (\pi/\lambda_j^2) [q_i(j+1) - q_i(j)]^2 \right\} - (\beta/J) \sum_{j=1}^J U\{q_i(j)\} \right], \end{aligned} \quad (11)$$

where  $q_i(1) = P_G(q_i(J+1))$  are the "classical" partition functions for the  $G$  set of linked trajectories,  $P_G$  is any permutation of the class  $G$ , and  $\lambda_j = \lambda/\sqrt{j}$  is the "high-temperature" thermal wavelength. Factors  $n(G)$ ,  $K(G)$ , and  $\text{sgn}(G)$  are calculated according to (7)–(9).

### C. Distribution over projections and values of the total spin

Since, for each closed linked trajectory, spin projections of all particles are the same and in the absence of an external field are either  $+\frac{1}{2}$  or  $-\frac{1}{2}$  with equal probability, it is not difficult to build a distribution over the value of the total spin projection (the sum of spin projections of all the particles). For a given diagram of the  $G$  class the full spin-projection distribution  $\omega(m, G)$  is determined by an evident formula:

$$\begin{aligned} \omega(m, G) &= \sum_{\sigma_1, \dots, \sigma_N = \pm \frac{1}{2}} \delta(\sigma_1, P_G(\sigma_1)) \cdots \delta(\sigma_N, P_G(\sigma_N)) \\ &\quad \times \delta \left[ \sum_{i=1}^N \sigma_i - m \right]. \end{aligned} \quad (12)$$

Practically, the distribution coefficients  $\omega(m, G)$  can be obtained as the number of ways to obtain  $m$ , adding up numbers  $\nu/2$  corresponding to all closed linked trajectories in the class  $G$  with various possible combinations of signs.

For the identical permutation  $\{C_\nu\} = \{N, 0, \dots, 0\}$  spin projections of all particles can have independent values  $\pm \frac{1}{2}$ . To obtain the full projection  $m$  it is necessary that  $N/2 + m$  particles should have spin projection  $+\frac{1}{2}$  and  $N/2 - m$  have  $-\frac{1}{2}$ . It can be fulfilled in  $C_N^{N/2+m}$  ways, i.e.,

$$\omega(m, 1) = C_N^{N/2+m} = \frac{N!}{(N/2+m)!(N/2-m)!}.$$

As an example of the general case for the diagram  $G$ , Fig. 2,  $N=6$ , one can get the following spin-projection distribution (see Table II):

$$\begin{aligned} \omega(m, G) &= (1, 1, 1, 2, 1, 1, 1) \\ m &= (-3, -2, -1, 0, 1, 2, 3) \end{aligned}$$

The total spin of the  $N$ -electron system  $S$  can have values in the interval from  $N/2$  up to  $\frac{1}{2}$  or 0 (depending

on the parity of  $N$ ) with step 1. Each state of spin  $S$  is  $2S+1$  times degenerate over the spin projection  $m = -S, \dots, S$ , each spin projection corresponding to a single microstate. It allows one to obtain the distribution  $\Omega(S, G)$  over values of the total spin  $S$  on the basis of the already existing distribution  $\omega(m, G)$  over  $m$ . Since each of the states with total spin  $S = m, m+1, \dots, N/2$  makes a single contribution to the set of states with total spin projection  $m$ , it is possible to write

$$\omega(m, G) = \sum_{S=m}^{N/2} \Omega(S, G)$$

and hence

$$\Omega(S, G) = \omega(S, G) - \omega(S+1, G) \quad (13)$$




(considering that  $\omega(N/2+1, G) = 0$ ). For cases presented before we have (a) for identical permutation:

$$\begin{aligned} \Omega(S, 1) &= C_N^{N/2+S} - C_N^{N/2+S+1} \\ &= \frac{N!(2S+1)}{(N/2-S)!(N/2+S+1)!} \end{aligned} \quad (14)$$

and (b) for the diagram in Fig. 2:

$$\Omega(3, G) = \Omega(0, G) = 1, \quad \Omega(2, G) = \Omega(1, G) = 0.$$

TABLE II. An example of the calculation scheme for the coefficients  $\omega(m, G)$  corresponding to the diagram of Fig. 2. The various spin-projection signs for each closed trajectory are listed.

Cycles				Total spin
$\nu$	3	2	1	projection
	+	+	+	3
	+	+	-	2
	+	-	+	1
	-	+	+	0
	+	-	-	0
	-	+	-	-1
	-	-	+	-2
	-	-	-	-3

In general  $\Omega(S, G)$  can be negative.

The coefficients  $\omega(m/G)$  and  $\Omega(S, G)$  determined by formulas (12) and (13) must evidently fulfill the following conditions:

$$K(G) = \sum_{m=-N/2}^{N/2} \omega(m, G) = \sum_{S=0 \text{ or } \frac{1}{2}}^{N/2} \Omega(S, G)(2S+1). \quad (15)$$

Now using (15) one can present the partition function with explicit contribution of states with different total spin:

$$Z = \frac{1}{N!} \sum_S (2S+1) \sum_G n(G) \text{sgn}(G) \Omega(S, G) Z_{cl}(G). \quad (16)$$

Formula (16) allows one to obtain canonical averages of quantities depending on spin. For instance,

TABLE III. Coefficients for the diagrams,  $N=2, 3, 4, 5$ .

$\{C_v\}$	Diagram	$n(G)$	$K(G)$	$\text{sgn}(G)n(G)K(G)$	$\omega(m, G)$	$\Omega(S, G)$		$\text{sgn}(G)n(G)(2S+1)\Omega(S, G)$			
						$S=1$	$S=0$	$S=1$	$S=0$		
$N=2$											
(2,0)		1	4	4	(1,2,1)	1	1	3	1		
(0,1)		1	2	-2	(1,0,1)	1	-1	-3	1		
$N=3$											
$\{C_v\}$	Diagram	$n(G)$	$K(G)$	$\text{sgn}(G)n(G)K(G)$	$\omega(m, G)$	$\Omega(S, G)$		$\text{sgn}(G)n(G)(2S+1)\Omega(S, G)$			
						$S=\frac{3}{2}$	$S=\frac{1}{2}$	$S=\frac{3}{2}$	$S=\frac{1}{2}$		
(3,0,0)		1	8	8	(1,3,3,1)	1	2	4	4		
(1,1,0)		3	4	-12	(1,1,1,1)	1	0	-12	0		
(0,0,1)		2	2	4	(1,0,0,1)	1	-1	8	-4		
$N=4$											
$\{C_v\}$	Diagram	$n(G)$	$K(G)$	$\text{sgn}(G)n(G)K(G)$	$\omega(m, G)$	$\Omega(S, G)$			$\text{sgn}(G)n(G)(2S+1)\Omega(S, G)$		
						$S=2$	$S=1$	$S=0$	$S=2$	$S=1$	$S=0$
(4,0,0,0)		1	16	16	(1,4,6,4,1)	1	3	2	5	9	2
(2,1,0,0)		6	8	-48	(1,2,2,2,1)	1	1	0	-30	-18	0
(0,2,0,0)		3	4	12	(1,0,2,0,1)	1	-1	2	15	-9	6
(1,0,1,0)		8	4	32	(1,1,0,1,1)	1	0	-1	40	0	-8
(0,0,0,1)		6	2	-12	(1,0,0,1)	1	-1	0	-30	18	0
$N=5$											
$\{C_v\}$	Diagram	$n(G)$	$K(G)$	$\text{sgn}(G)n(G)K(G)$	$\omega(m, G)$	$\Omega(S, G)$				$\text{sgn}(G)n(G)(2S+1)\Omega(S, G)$	
						$S=\frac{5}{2}$	$S=\frac{3}{2}$	$S=\frac{1}{2}$	$S=\frac{5}{2}$	$S=\frac{3}{2}$	$S=\frac{1}{2}$
(5,0,0,0,0)		1	32	32	(1,5,10,10,5,1)	1	4	5	6	16	10
(3,1,0,0,0)		10	16	-160	(1,3,4,4,3,1)	1	2	1	-60	-80	-20
(1,2,0,0,0)		15	8	120	(1,1,2,2,1,1)	1	0	1	90	0	30
(2,0,1,0,0)		20	8	160	(1,2,1,1,2,1)	1	1	-1	120	80	-40
(0,1,1,0,0)		20	4	-80	(1,0,1,1,0,1)	1	-1	1	-120	80	-40
(1,0,0,1,0)		30	4	-120	(1,1,0,0,1,1)	1	0	-1	-180	0	60
(0,0,0,0,1)		24	2	48	(1,0,0,0,0,1)	1	-1	0	144	-96	0

$$\langle \hat{S}^2 \rangle = \frac{1}{ZN!} \sum_S S(S+1)(2S+1) \times \sum_G n(G) \text{sgn}(G) \Omega(S, G) Z_{cl}(G). \quad (17)$$

In Table III we present all the diagrams and coefficients  $n(G)$ ,  $K(G)$ ,  $\omega(m, G)$ , and  $\Omega(S, G)$  for  $N=2, 3, 4, 5$ .

It seems that the coefficients  $\omega(m, G)$  and  $\Omega(S, G)$  can also be obtained using group theory and the Young diagrams [8,10]. One can notice [11] that, for each  $N$ ,  $\omega(m, G)$  coincide with the characters of representations and  $\Omega(S, G)$  with the character of irreducible representations of the group of permutations for corresponding classes  $G$ .

Calculation of the coefficients on the basis of Young diagrams was made in [8], but our results for  $\Omega(S, G)n(G)\text{sgn}(G)$  differ from those of the paper [8] by factors  $\Omega(S, 1)$  [see (14) and the first line for each  $N$  in Table III]. The complete agreement with [8] is for  $N=2$ ; for  $N \geq 3$  it is only for  $S=S_{\max}$  since  $\Omega(S_{\max}, G)=1$  for all  $N$  and  $G$ .

Meanwhile, the necessity of factors  $\Omega(S, 1)$  can be confirmed by some evident considerations. In the high-temperature limit only the identical permutation survives and the spin contribution to the partition function is  $\sum_{0 < S < N/2} \Omega(S, 1)(2S+1)$ . It must be equal to  $2^N$ . It is really so only if  $\Omega(S, 1)$  are determined according to Table III. The average  $\langle \hat{S}^2 \rangle$  for the whole system as  $\beta \rightarrow 0$  is

$$\langle \hat{S}^2 \rangle = \sum_{0 < S < N/2} (2S+1)S(S+1)\Omega(S, 1)/2^N$$

and it must give the classical limit  $3N/4$  for  $N$  independent spins. It is valid indeed if  $\Omega(S, 1)$  are determined as in Table III.

### III. ORGANIZATION OF THE MC PROCEDURE

As seen from (10), the complete partition function includes integration over all vertices of the trajectories  $q_i(j)$  and summation over diagrams (classes). Accordingly the MC random walk in the space of states must include two types of steps: changes of coordinates and changes of diagram, i.e., linkage of trajectories (such an algorithm for the  $N$ -electron system was presented and realized in [7,8]). The first type of step presents no problem and can be carried out according to conventional rules (Metropolis procedure for classical systems). Problems arise for MC steps of the second type. There are two main problems.

The first is the problem of MC transitions between diagrams, i.e., between different types of trajectory linkages. The following procedure was suggested in [8]. A pair of "simultaneous" points are chosen arbitrarily on two different trajectories:  $q_i(j)$  and  $q_k(j)$ . Then follows "rethrowing" of links: from  $q_i(j)$  to  $q_k(j+1)$  and from  $q_k(j)$  to  $q_i(j+1)$ . As is easily seen, rethrowing of links between trajectories belonging to different cycles results in their unification and, between trajectories inside a common cycle, to its disruption into two cycles. This

way it is possible to obtain all possible topological classes of trajectories.

However, there arises a difficulty. Usually points  $q_i(j)$  and  $q_k(j+1)$  are far from each other and the emergence of two new terms proportional to  $[q_i(j) - q_k(j+1)]^2$  results most often in a very low transition probability, the more so at high temperatures.

The second problem concerns the fact that weight factors in (10) have alternating signs. This obstacle is avoided by ascribing a negative sign to the averaged quantity (estimator) and dividing the sum obtained by the counter which contains a sum of  $+1$  and  $-1$ ,  $-1$  corresponding to states with negative sign [7]. If it occurs that contribution from diagrams (classes) with positive and negative weights are equal (or even approximately equal) the uncertainty  $0/0$  emerges. Unfortunately this is the case when the PIMC method is applied to electron systems such as atoms and molecules at room temperature when the number of electrons exceeds  $N=2$ . Room temperatures are low for such systems. At temperatures tending to zero the harmonic term  $[Jm/(2\beta h^2)][q_i(j) - q_i(j+1)]^2$  in (6) also tends to zero, leading to the "equivalence" of different diagrams. The sum of all weights corresponding to different diagrams (see Table III) is zero for  $N \geq 3$ . As a result in practical calculations the counter would contain a number like several hundred after millions of MC steps.

As shown in a number of papers (e.g., [13,14]):

$$\frac{Z_+ - Z_-}{Z_+ + Z_-} \sim \exp[-\beta(E_0 - E_b)] \quad (18)$$

as  $T \rightarrow 0$  ( $\beta \rightarrow \infty$ ). Here  $Z_+$  and  $Z_-$  are (positive) contributions to the partition function with positive and negative weight and  $E_b$  and  $E_0$  are the energies of the ground state for boson and fermion systems, respectively.

In [13] the following approach to overcoming this uncertainty was suggested. It is known that the solution of the Schrödinger equation at lowest energy is symmetrical under transpositions of particles. Let this energy be  $E_b$ , which corresponds to the ground state of a boson system. For fermions the wave function is antisymmetric (at least for  $N \geq 3$ ) and the ground-state energy  $E_0 > E_b$ . In the process of simulation we, in fact, reproduce the partition function  $Z_+ + Z_-$  corresponding to an  $N$ -particle boson system thus involving in our game all states with energies  $E > E_b$ , including  $E < E_0$ . These nonphysical states are indeed eliminated by the "alternative sign" weight.

It was shown in [13] (which is easy to understand) that

$$\gamma_+(U) = \gamma_-(U) \quad \text{for } U < E_0, \quad (19)$$

where  $\gamma_+(U)$  and  $\gamma_-(U)$  are energy densities for states with positive and negative weights. At low temperatures the system mainly occupies states in the vicinity of  $E_b$  with  $E < E_0$ . These states cancel and yield no contribution to the average. Therefore one should try to construct a computational scheme which avoids states with  $E < E_0$ . Such an approach was suggested in [13] for the Hubbard model.

In our case such an approach cannot be applied since in the coordinate representation used in the path-integral

simulations the energy has no definite value (the kinetic part of the Hamiltonian does not commute with the position operator). Formally one can write an estimator for  $U$  but it would depend on  $\beta$ . As a result  $\gamma_+(U)$  and  $\gamma_-(U)$  would also include  $\beta$  and the arguments leading to (19) become incorrect.

We propose another scheme which permits one to attack the problem of sign. Let us represent the exponent in (11) as a sum of two terms:

$$H_T(q) = \frac{1}{J} \sum_{j=1}^J U\{q_i(j)\} + \sum_{j=1}^{J-1} \sum_{i=1}^N \frac{Jm}{2\beta^2\hbar^2} [q_i(j+1) - q_i(j)]^2 \quad (20)$$

$[H_T(q)$  does not depend on permutation class  $G$ ]. The remaining part is

$$H_{ex}(q, G) = \sum_{i=1}^N \frac{Jm}{2\beta^2\hbar^2} [q_i(J) - q_{P_G(i)}(1)]^2. \quad (21)$$

It is then possible to express  $Z$  (10) as follows:

$$\begin{aligned} Z &= \frac{1}{N!} \sum_G \int \prod_{i=1}^N \prod_{j=1}^J dq_i(j) (\lambda_j)^{-3JN} \text{sgn}(G) n(G) K(G) \\ &\quad \times \exp[-\beta(H_T(q) + H_{ex}(q, G))] \\ &= \frac{1}{N!} \int \prod_{i=1}^N \prod_{j=1}^J dq_i(j) (\lambda_j)^{-3JN} \\ &\quad \times \exp[-\beta H_T(q)] W(q), \end{aligned} \quad (22)$$

where

$$W(q) = \sum_G \text{sgn}(G) n(G) K(G) \exp[-\beta H_{ex}(q, G)]. \quad (23)$$

So summation over diagrams can be carried out explicitly for each configuration and consequently there is no need to make a random walk in the space of diagrams, as was the case in [8].

The factor  $W\{q_i(j)\}$  can be now included in the potential in the following way:

$$\begin{aligned} Z &= \int \prod_{i=1}^N \prod_{j=1}^J dq_i(j) (\lambda_j)^{-3JN} \text{sgn}[W(q)] \\ &\quad \times \exp[-\beta H_T(q) + \ln|W(q)|]. \end{aligned} \quad (24)$$

So we simulate a system of  $N$  nonclosed trajectories with the inclusion of an additional potential  $|W\{q_i(j)\}|$ , which accounts for the contribution of all types of linkage schemes and depends only on the end points of the trajectories.

There is hope that an essential part of the uncertainty would cancel in the sum of diagrams. For  $\beta \rightarrow \infty$ ,

$$W(q) \rightarrow \sum_G \text{sgn}(G) n(G) K(G) = 0.$$

In this way we explicitly distinguish the factor which results in  $Z \rightarrow 0$ .

#### IV. TEST SIMULATION: FOUR ELECTRONS IN A CAVITY

We have tested our approach for a comparatively simple system: four electrons in a spherical cavity of radius 1 nm with no external field. The absence of the strong attractive field of an atomic nucleus allows us to make calculations with a comparatively small number of vertices  $J$ —about several tens for each electron (see also [7]). In this work we use  $J = 64$ .

To simulate the ensemble with the partition function (24) it is sufficient (in principle) to make MC steps of only one type—shifts of single vertices. However, as became clear from preliminary MC runs, such a primitive procedure proves to be ineffective. Really, due to the presence of the effective potential  $\ln|W(q)|$ , the trajectories tend to become closed. Although all the linkages are present only one term in the sum (23) yields a predominant contribution. Regions of the configurational space corresponding to different linkage schemes appear to be separated by high-potential barriers. So in the course of simulation, transitions from one such region to another occur extremely rarely.

In order to achieve good averaging in the whole space of states during a MC run we introduce three additional types of steps: (1) shift of a whole trajectory; (2) cyclical permutation of vertices [in fact, it means that the function  $W(q)$  is calculated between vertices labeled “ $j$ ” and “ $j+1$ ,” rather than between the “ends” of trajectories labeled as “1” and “ $J$ ”; “ $j$ ” is chosen arbitrarily]; (3) exchange of a pair of particles within parts of trajectories  $\{q_i(j)\} \leftrightarrow \{q_k(j)\}$  for  $j_0 < j < j_1$ , under the condition that  $W(q)$  is calculated between points  $j_0 - 1$  and  $j_0$ .

The latter transition yields as a rule an effective rethrowing of the system “across the barrier”—to the region of states corresponding to the predominant contribution of another diagram. Application of such an algorithm provided a quite reliable sampling covering all significant areas of the configurational space.

In our calculations standard estimators for potential and kinetic energies were used:

$$\begin{aligned} E_p &= \frac{1}{J} \sum_{j=1}^J U\{q_i(j)\}, \\ E_k &= \frac{3JN}{2\beta} - \frac{\pi}{\beta\lambda_j^2} \sum_{i=1}^N \sum_{j=1}^J [q_i(j) - q_i(j+1)]^2. \end{aligned}$$

To obtain quantities determined by spin we calculated contributions to the partition functions from each diagram:

$$\begin{aligned} \rho(G) &= \frac{Z_{cl}(G)}{Z_+ + Z_-} = \frac{1}{(Z_+ + Z_-)\lambda_j^{3JN}} \int \prod_{i,j} dq_i(j) \exp[-\beta(H_T(q) + H_{ex}(q, G))] \frac{W_+(q)}{W_+(q)} \\ &= \frac{\left\langle \frac{\exp[-\beta H_{ex}(q, G)]}{W_+(q)} \right\rangle_+}{\sum_G n(G) K(G) \left\langle \frac{\exp[-\beta H_{ex}(q, G)]}{W_+(q)} \right\rangle_+}, \end{aligned} \quad (25)$$

where  $n(G)$  and  $K(G)$  are taken from Table III,  $W_+$  is expressed as (22) with omitted  $\text{sgn}(G)$  and  $\langle \rangle_+$  is averaging with the non-negative weight function

$$\sum_G n(G)K(G)\exp[-\beta(H_T(q) + H_{\text{ex}}(q, G))]/(Z_+ + Z_-),$$

and  $Z_{\text{cl}}(G)$  is the "classical" partition function for the diagram  $G$  [see (11)]. Now using Table III it is easy to calculate contributions to states with given values of the total spin  $S$ :

$$\rho(S) = \sum_G \text{sgn}(G)n(G)(2S+1)\Omega(S, G)\rho(G). \quad (26)$$

$\rho(S)$  can then be used to calculate the average square of the spin operator  $\langle \hat{S}^2 \rangle$  and the zero-field spin magnetic susceptibility (we do not touch upon the question of the orbital momentum):

$$\langle \hat{S}^2 \rangle = \sum_S S(S+1)\rho(S),$$

$$\chi = \beta \langle \hat{S}^2 \rangle.$$

To test the program we repeated some results for a system of two electrons in a spherical cavity of the same radius (1 nm) obtained earlier in [7] with the aid of another algorithm. For  $T=439$  K values of the potential and kinetic energies  $E_p = 1.25 \pm 0.01$  eV and  $E_k = 0.75 \pm 0.01$

eV were obtained, coincident with those of [7].

Results for the four-electron system [potential and kinetic energies, diagram contribution  $\rho(G)$ , and some others] are given in Table IV. Radial distributions of electron density at different temperatures are shown in Fig. 3.

Lengths of Markov chains were  $(30-60) \times 10^6$  MC steps (see Table IV; a MC step is either an attempt to move a single vertex of any trajectory or a special step of the type 1-3). The first  $10^7$  steps were excluded from averaging. After that each 100th configuration was averaged. The statistical error was determined from the dispersion of results averaged over Markov chain intervals of  $5 \times 10^6$  steps.

To possibly achieve faster equilibrium of the system, the initial trajectories were created in the manner of the Rosenbluth algorithm [15] for polymer simulations: each vertex  $q_i(j+1)$  was obtained by addition of a vector  $dq$  to the point  $q_i(j)$ , the length of  $dq$  being made equal to the average distance between neighboring vertices for free particles at a given temperature:

$$dq^2 = \lambda^2 / (2\pi J).$$

The most accurate results were obtained for the energy (error 2-3 %). Radial distribution functions are less accurate, especially for low temperatures (error 15-20 %).

TABLE IV. Results of PIMC simulation of the four-electron system in the spherical cavity.

Quantity	T (K)	300	500	1000	2000	Classical limit
Energies (eV)						
$E_p$		7.5±0.2	7.81±0.1	7.89±0.1	8.24±0.07	
$E_k$		2.2±0.2	2.34±0.1	2.88±0.1	3.32±0.2	
$E_k/(3NkT/2)$		14	9	5.8	3.1	1
$U = E_p + E_k$		9.7±0.3	10.15±0.10	10.77±0.10	11.56±0.20	
Diagram contribution $\rho(G)$						
(4,0,0,0)		0.0117	0.0185	0.035	0.051	$\frac{1}{16}$
(2,1,0,0)		0.0082	0.0071	0.0061	0.0036	0
(0,2,0,0)		0.0065	0.005	0.0025	0.0002	0
(1,0,1,0)		0.008	0.0071	0.0026	0.0003	0
(0,0,0,1)		0.0074	0.0062	0.003	0	0
Weighted diagram contributions $n(G)K(G)\rho(G)$						
(4,0,0,0)		0.18	0.30	0.56	0.82	1
(2,1,0,0)		0.39	0.34	0.29	0.17	0
(0,2,0,0)		0.078	0.06	0.03	0.002	0
(1,0,1,0)		0.26	0.23	0.085	0.008	0
(0,0,0,1)		0.09	0.075	0.036	0	0
Contribution to spin states $\rho(S)$						
$\rho(0)$		0.0±0.2	0.05±0.15	0.2±0.1	0.15±0.05	$\frac{2}{16}$
$\rho(1)$		0.8±0.2	0.65±0.15	0.7±0.1	0.60±0.05	$\frac{9}{16}$
$\rho(2)$		0.2±0.2	0.30±0.15	0.10±0.15	0.25±0.05	$\frac{5}{16}$
$\langle \hat{S}^2 \rangle$		2.8	3	2.3	3	3
Other quantities						
$\langle \text{sgn}[W(q)] \rangle$		0.04±0.02	0.19±0.03	0.31±0.05	0.68±0.05	1
Total MC steps in units of $10^6$		60	50	30	30	



Even greater is the error for the spin distribution  $\rho(S)$  since it is a result of a very delicate balance of various diagram contributions. Still, it can be noted that with decreasing of temperature the proportion of states with total spin  $S=1$  grows. It could probably indicate that the ground state of the system has such a total spin.

At the highest temperature (2000 K) the first diagram (identical permutation) makes the main contribution to the partition function (more than 80%). The spin contribution  $\rho(S)$  becomes close to the classical one as well as the mean square of spin:  $\langle \hat{S}^2 \rangle = 4 \times \frac{3}{4}$ . One can say that electrons in the cavity at this temperature behave almost as distinguishable particles. However, quantum effects are still strong: the kinetic energy per particle remains much higher than  $3kT/2$ ; the radial distribution function falls near the wall of the sphere (in the classical limit it must be maximum at the wall due to repulsion of electrons). An analogous behavior was observed also for two electrons in [7].

The radial distribution function appears to be very weakly dependent on temperature: an almost sevenfold decrease of temperature yields a rather weak shift of the maximum toward the wall. It can be explained by the fact that two factors—Coulomb repulsion and quantum effects (“exchange forces”)—act in opposite manner with changing temperature.

## V. CONCLUSION

Calculations performed above demonstrate the possibility of *ab initio* simulation of a many-electron system with strict account of permutation symmetry and spin statistics, though our hopes to resolve the sign problem by summing the diagrams at each configuration in (23) were justified only partially. As a rule in the sum (23) for  $W(q)$  only one term dominates and there occurs no

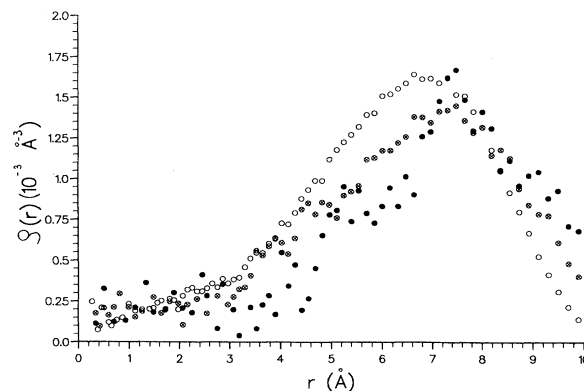


FIG. 3. Radial distribution of the electron density for various temperatures: ●,  $T = 300$  K; ◻,  $T = 500$  K; ○,  $T = 2000$  K.

effective contraction of different diagram contributions. However, the proper algorithm (inclusion of steps 1–3) still makes it possible to simulate such systems up to comparatively low temperatures even on a personal computer.

The proposed method can be applied without considerable increase of computer time to an electron system in a weak external field, e.g., free or weakly coupled external electrons of atoms and molecules in the effective field of the remaining ions, electron component in electrides and alkalides [16], etc. The simulation of the complete set of electrons in an atom or a molecule would require essentially greater efforts; in the strong field of a nucleus one should account for a very great number of vertices: thousands or maybe more. Moreover, strongly coupled states imply an effective decrease of temperature that makes the sign problem even more serious.

- 
- [1] R. P. Feynman and A. R. Hibbs, *Quantum Mechanics and Path Integrals* (McGraw-Hill, New York, 1965).  
 [2] L. D. Fosdick and H. F. Jordan, *Phys. Rev.* **143**, 58 (1966).  
 [3] J. A. Barker, *J. Chem. Phys.* **70**, 2914 (1979).  
 [4] M. F. Herman, E. J. Bruskin, and B. J. Berne, *J. Chem. Phys.* **76**, 5150 (1982).  
 [5] C. L. Cleveland, U. Landman, and R. N. Barnett, *Phys. Rev. B* **39**, 117 (1989).  
 [6] S. V. Shevkunov, *Teplofiz. Vys. Temp.* **28**, 1 (1990) [*High Temp. (USSR)* **28**, 1 (1990)].  
 [7] S. V. Shevkunov and P. N. Vorontsov-Velyaminov, *Mol. Simul.* **7**, 249 (1991).  
 [8] S. V. Shevkunov, *Inst. Theor. Phys. Report No. ITF-87-105E*, Kiev, 1987 (unpublished).  
 [9] R. P. Feynman, *Statistical Mechanics* (Benjamin, New

- York, 1972).  
 [10] L. D. Landau and E. M. Lifshits, *Quantum Mechanics. Nonrelativistic Theory* (Nauka, Moscow, 1989).  
 [11] J. P. Elliot and P. G. Dawber, *Symmetry in Physics* (Macmillan, London, 1979).  
 [12] I. A. Favorskii, A. P. Lyubartsev, I. V. Roshdestvenskii, and A. G. Gutman, *Inst. Theor. Phys. Report No. ITF-85-94R*, Kiev, 1985 (unpublished).  
 [13] I. Morgenstern, *Z. Phys. B* **77**, 267 (1989).  
 [14] W. H. Newman and A. Kuki, *J. Chem. Phys.* **96**, 1409 (1992).  
 [15] M. N. Rosenbluth and A. W. Rosenbluth, *J. Chem. Phys.* **23**, 356 (1955).  
 [16] J. L. Dye and M. G. De Backer, *Annu. Rev. Phys. Chem.* **38**, 271 (1987).